ACS OMEGA

Open Access

http://pubs.acs.org/journal/acsodf

Article

Cooling Performance of TiO_2-Based Radiative Cooling Coating in Tropical Conditions

Bhrigu Rishi Mishra,[‡] Sreerag Sundaram,[‡] and Karthik Sasihithlu*

Cite This: *ACS Omega* 2024, 9, 49494−49502

Read Online

ACCESS | Metrics & More | Article Recommendations | Supporting Information

ABSTRACT: The cooling power of radiative cooling (RC) coatings depends not only on the radiative properties of the coating but also on environmental variables. In tropical environments, the cooling performance of RC coatings deteriorates due to high humidity and high solar radiation. Previous studies focused on developing high solar-reflective coatings to achieve subambient cooling in tropical environments. However, these coatings have not demonstrated the ability to be used at a large scale, mainly due to their high cost or less durability. Herein, we test an RC paint coating composed of TiO_2 and polydimethylsiloxane (PDMS) in three different cities with high and moderate humidity levels. Though a significant reduction in the internal temperature of an RC paint-coated aluminum (Al) box is observed, compared to an uncoated Al box, in both high and moderate humidity environments, subambient cooling is not achieved. A comprehensive analysis is conducted to clarify the reasons behind the inability to attain subambient cooling.

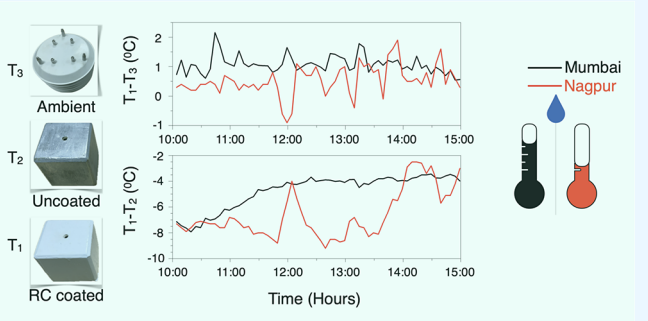

1. INTRODUCTION

As the global climate crisis continues to escalate, there is an urgent need for innovative and sustainable solutions to mitigate the adverse effects of rising temperatures and reduce energy consumption. In this pursuit, radiative cooling (RC) coatings have emerged as a promising avenue for enhancing passive cooling strategies in various applications, ranging from buildings[1,2] and automobiles[3] to electronic devices.[4] These specialized coatings offer a sustainable and clean cooling solution to counteract the urban heat island effect and reduce the dependence on energy-intensive air conditioning systems. Apart from effectively reflecting incoming solar radiation, these coatings are engineered to release thermal radiation in the long-wavelength infrared (LWIR) spectrum. This LWIR radiation has the unique ability to pass through the Earth's atmosphere via the transparency window, which spans the 8−13 μm wavelength range, and subsequently disperse into the cold depths of outer space. This phenomenon, known as passive radiative cooling, allows surfaces coated with such coatings to cool significantly below ambient temperatures, even in the midst of intense sunlight. Theoretically, it can potentially reduce the temperature of a surface, passively, by up to 60 °C.[5] Recent review articles[6,7] have detailed the progress on radiative cooling coating designs and materials. Different types of structures have been explored, such as multilayer,[8] glass-polymer hybrid metamaterial,[9] biologically inspired structures,[10,11] hierarchical porous polymer,[12] and disordered coatings,[2,13−17] aiming to achieve the desired radiative properties in the respective spectral bands. Among these, disordered or paint coatings have gained popularity due to their simple design, ease of fabrication, and low cost. Recent studies have also emphasized the importance of considering practical aspects of RC coatings, such as durability and scalability, while maintaining high cooling performance.[18,19]

The evaluation of the performance of such coatings is predominantly based on their solar reflectivity and infrared (IR) emissivity. While these indicate the material's potential to cool a coated surface, it is crucial to note that prevailing environmental conditions during outdoor testing also significantly influence the cooling performance of these coatings. One of the mechanisms by which an RC coating provides cooling is by enabling an IR radiative exchange with cold outer space via the atmospheric transparency window (ATW), which is heavily affected by local humidity. Researchers have previously studied the impact of environmental conditions like humidity, ambient temperature, and cloud cover on the cooling performance of an RC coating in different locations.[20−24] It is evident that transmissivity of the atmosphere in the 8−13 μm wavelength range is significantly lower in regions with high humidity.[23] This makes achieving

Received: August 6, 2024
Revised: October 4, 2024
Accepted: November 25, 2024
Published: December 4, 2024

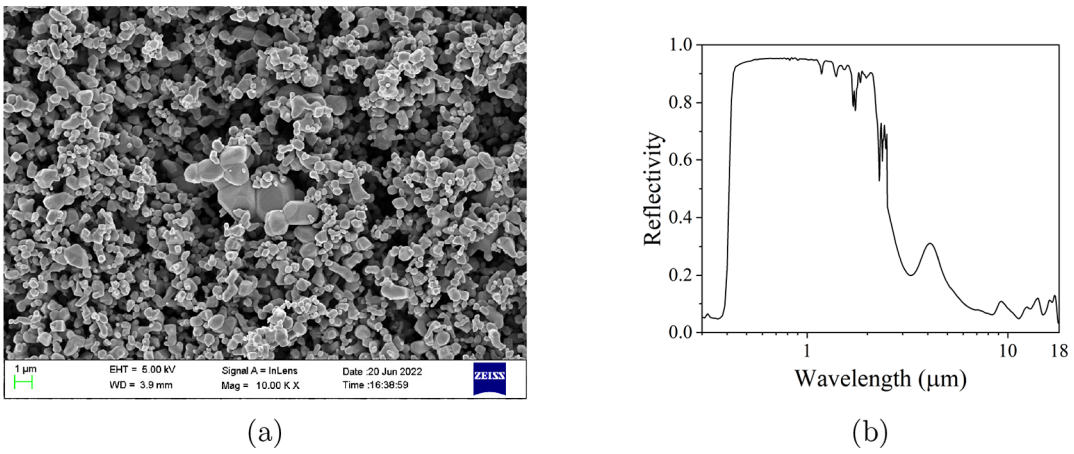

Figure 1. (a) SEM image of the TiO_2 pigment. The TiO_2 particle radius distribution is 0.255 μm ± 0.13 μm (b) Measured reflectivity of a 280 μm-thick fabricated paint coating with a TiO_2 pigment volume concentration of 15%.

subambient cooling highly challenging in tropical areas that are characterized by high solar radiation and high humidity. A study conducted in Hong Kong[25] showcased the inability to achieve daytime subambient cooling despite using a coating with high solar reflectivity (95%) and high ATW emissivity (98%). In order to achieve subambient cooling in these highly humid environments, recent studies have highlighted the need to develop RC coatings with ultrahigh solar reflectivities. An expanded polytetrafluoroethylene (ePTFE) film and a Ag layer deposited on a transparent glass substrate, with a solar reflectivity and ATW emissivity of 98% and 86% respectively, showed subambient cooling of up to 2.7 °C in Hong Kong.[26] A subambient cooling of 0.9 °C was achieved by a porous polymer coating[27] with a solar reflectivity of 94% and an ATW emissivity of 97% in Shanghai, China, where the solar radiation intensity and relative humidity are about 930.7 W/m^2 and 49% respectively. Another study in Singapore[28] demonstrated subambient cooling of 1.5 °C under a solar irradiance of 1000 W/m^2 and an atmospheric radiation of 480 W/m^2 on a clear day using a $BaSO_4$/P(VDF-HFP) coating with 97% solar reflectivity and 94.2% ATW emissivity.

Although these coatings, designed for tropical environments, have shown promising cooling capabilities, their scalability and cost-effectiveness remain significant challenges, hindering widespread adoption. For example, the inclusion of a thin film of silver not only raises the overall cost but also diminishes the coating's visual appeal; porous polymer coatings are yet to demonstrate rapid commercial scalability[29]; and the use of low-refractive-index pigments in high volume fractions adversely impacts coating properties such as stress/strain tolerance, water resistance, and durability due to the reduced concentration of polymer binders.[30] In order to obtain high reflectivity using paint coating, materials with high band gaps and low refractive indices such as SiO_2,[13] $BaSO_4$,[2] $CaCO_3$,[14] and Al_2O_3[17] have been used with large volume fractions (>50%) to compensate for the low scattering caused by the small difference in refractive indices between these pigments and polymers (0.05−0.25). A high pigment volume concentration in paint implies a decreased polymer (binder) concentration and an increase in cost. Furthermore, beyond a certain pigment concentration, a coating becomes fragile, less ductile, and low in adhesive strength due to the development of internal stresses.[31,32] Thus, these compounds are typically used as auxiliary pigments to balance performance and economics in paint formulations. One approach to enhance durability in high-pigment films involves sandwiching the functional layer between protective top and bottom coats,[33] although its feasibility for coatings with pigment concentrations exceeding 50% remains to be explored. In this context, TiO_2-based coatings have stood out due to their excellent optical properties, ease of fabrication, and economic viability. Regardless of the low solar reflectivity due to UV absorption, TiO_2 is still being used in solar-reflective cool roof paints as well as in radiative cooling coatings[16,34−37] due to its high refractive index, enabling it to be used at low pigment volume concentrations in paint compositions. Various modifications for TiO_2-based coatings have been explored in the literature, including the incorporation of fluorescent pigments to reduce UV absorption,[16] the development of polymer-free coatings to eliminate NIR absorption,[34] and the use of hollow TiO_2 spheres, which have the potential to increase light scattering by enhancing the refractive index contrast.[38]

Despite the recognized potential of TiO_2-based radiative cooling paints, there is a dearth of comprehensive studies examining their performance under tropical conditions. Tropical regions, characterized by high ambient temperatures, high humidity, and intense solar irradiance, pose unique challenges and opportunities for the application of radiative cooling technologies. Understanding the effectiveness of TiO_2-based radiative cooling paints in such environments is crucial for optimizing their design and deployment. This study aims to bridge this gap by analyzing the cooling performance of TiO_2/PDMS radiative cooling paints under tropical conditions. In a previous study, we had designed a TiO_2/PDMS coating for use in radiative cooling applications,[39] which has been fabricated and tested in several other studies by other research groups.[35−37] Through a series of controlled experiments and field tests in three different locations, namely, Mumbai, Nagpur, and Prayagraj, we evaluate the paint's ability to reduce enclosure temperatures and enhance thermal comfort in tropical climates. Our findings provide valuable insights into the practical viability and efficiency of TiO_2-based radiative cooling paints, contributing to the development of scalable and sustainable cooling solutions for regions with high solar insolation.

In addition to this, we also review current practices in reporting experimental tests, viz. the use of radiation shields and polyethylene covers to minimize convective losses and the

https://doi.org/10.1021/acsomega.4c07223
ACS Omega 2024, 9, 49494−49502

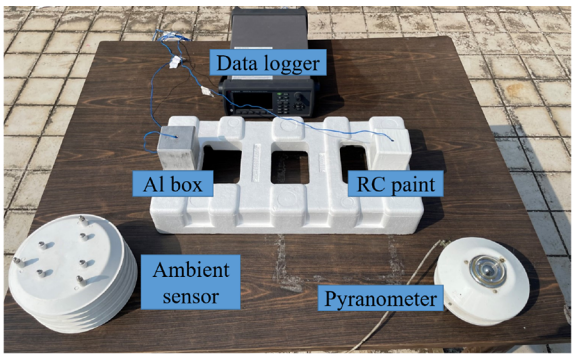

(a)

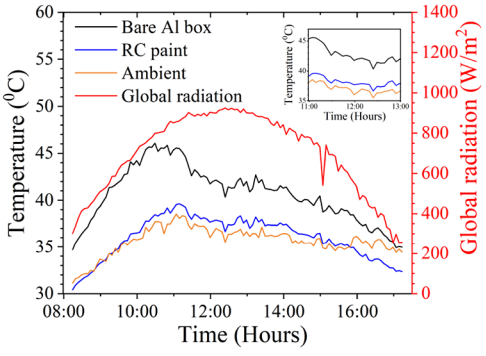

(b)

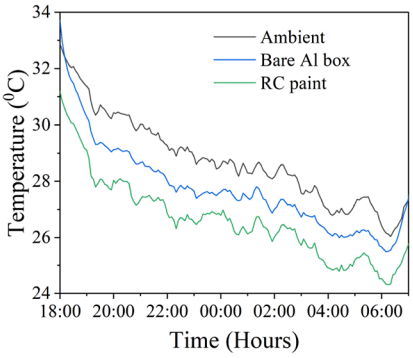

(c)

Figure 2. (a) Experimental setup to measure the cooling performance of RC coating comprising data logger, Stevenson screen (ambient sensor in image), pyranometer, and RC paint-coated and bare Al boxes. (b) Comparison of temperatures recorded within the enclosure space of the bare aluminum box, the one coated with RC paint, and the ambient temperature on April 25, 2023 during daytime and (c) during night-time. Global radiation levels, as measured by the pyranometer during daytime, are plotted on the right axis. The inset in (b) provides an enlarged view of the temperatures recorded during mid-day hours.

measurement of ambient temperature. It has been observed that certain practices may inadvertently increase the measured temperatures. For instance, the use of PE top covers, intended to minimize nonradiative losses and thus offer a clearer insight into radiative cooling efficiency, has been found to trap heat within the radiation shield box. Such accumulation of heat can elevate air temperatures to as high as 60−70 °C.[15,40] This heightened air temperature inside the box can exaggerate the subambient cooling effect when compared to tests conducted without a PE film covering the top. Two very recent publications[41,42] have also highlighted these issues. We expand on these works with the goal of promoting a unified methodology for reporting more accurate and comprehensive performance readings of novel radiative cooling coatings.

2. RESULTS AND DISCUSSION

The paint coating, as mentioned previously, utilizes TiO_2 as the primary pigment for achieving daytime radiative cooling. TiO_2 is chosen for its high refractive index, which enables high reflectivity in the visible and near-infrared (NIR) spectra, even at reduced volume concentrations (15% used in this study).[39] PDMS, known for its low solar absorption, biocompatibility, and hydrophobic properties, serves as the binder. Detailed information on the paint coating's design process can be found in Section S1 of the Supporting Information, along with the procedure used to fabricate the paint, which is outlined in Section 4.

2.1. Morphology of TiO_2 and Optical Properties of the Paint. The SEM image of the TiO_2 powder used in this work is shown in Figure 1a. The pigment particle radius distribution is observed to be 0.255 ± 0.13 μm. The reflectivity of our fabricated TiO_2/PDMS coating with a thickness of 280 μm is presented in Figure 1b. In the visible and NIR regions, the paint's reflectivity is observed to be greater than 94%, but absorption in the UV spectrum results in the net weighted solar reflectivity ($R_{solar} = [\int I_{AM1.5}(\lambda)\, R(\lambda)\, d\lambda]/[\int I_{AM1.5}(\lambda)\, d\lambda]$, where $I_{AM1.5}(\lambda)$ is the spectral solar irradiance[43]) of the fabricated coating to reduce to 88.2%. Increasing the thickness of the coating does not reveal any significant increase in reflectivity. The weighted emissivity in the ATW, calculated using $[\int I_{bb}(T = 300\ K, \lambda)\, \epsilon(\lambda)\, d\lambda]/[\int I_{bb}(T = 300\ K, \lambda)\, d\lambda]$, where I_{bb} is Planck's blackbody radiation and $\epsilon(\lambda) = 1 - R(\lambda)$ with $R(\lambda)$ being the reflectivity, is seen to be 92.4%.

2.2. Impact of Environmental Factors on Subambient Cooling. *2.2.1. Cooling Performance in High-Humid Conditions: Mumbai.* Many previously reported studies[12,15,44,45] assessed the cooling performance of RC coating on flat substrates by measuring the temperature of the coating relative to the ambient temperature. This approach does not mimic real-world scenarios where coatings are applied to structures to cool enclosed spaces. To better simulate real-world conditions, we evaluate the cooling efficiency of the RC paint when applied on a hollow 4 mm-thick aluminum box (7 cm × 7 cm × 7 cm) and measure its enclosure temperature, rather than the temperature of the coating. For the experiment,

https://doi.org/10.1021/acsomega.4c07223
ACS Omega 2024, 9, 49494−49502

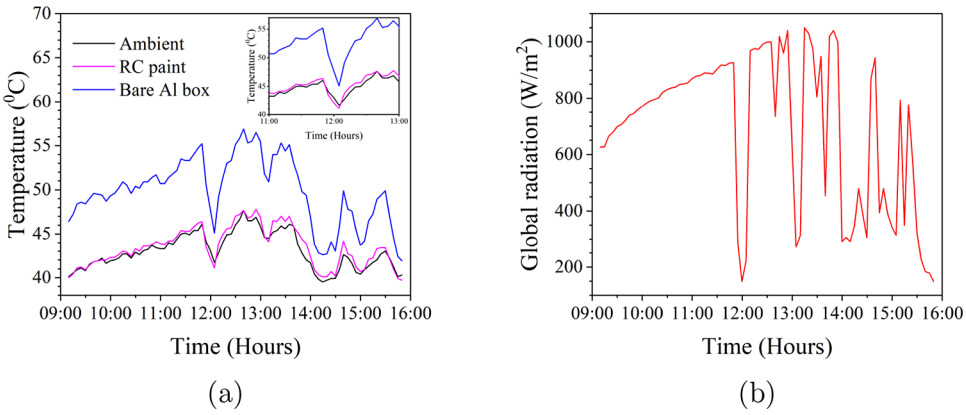

Figure 3. Temperature profile (a) and global radiation (b) recorded in Nagpur on June 12, 2023. The inset in (a) provides an enlarged view of the temperatures recorded during the mid-day hours.

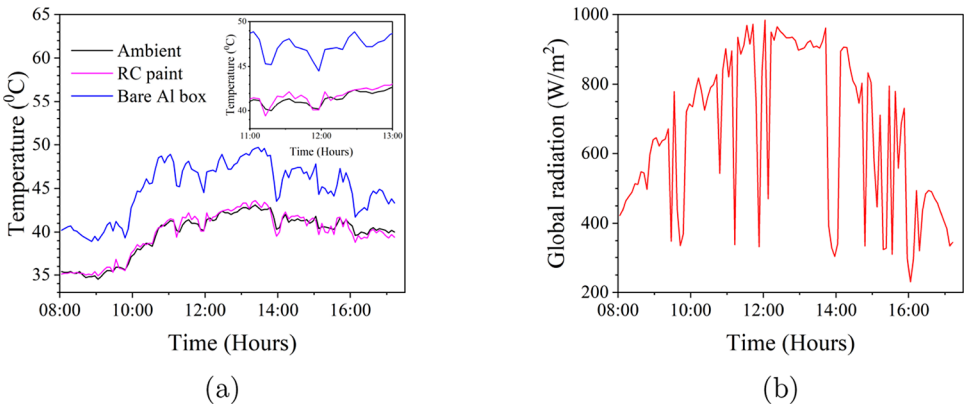

Figure 4. Temperature profile (a) and global radiation (b) recorded in Prayagraj on June 22, 2023. The inset in (a) shows a magnified view of the temperature curves during the mid-day hours.

we employed two aluminum boxes: one coated with TiO_2/PDMS paint (labeled as RC paint in figures) and an uncoated one as a control (labeled as bare Al box in figures). The experimental setup is shown in Figure 2a. Detailed information on experimental setup is given in Section 4. The outdoor experiments were conducted on the rooftop of the Department of Energy Science and Engineering at the Indian Institute of Technology Bombay, Mumbai. Mumbai is characterized by high humidity, with levels exceeding 80%.[22]

The cooling performance of the RC paint coated on the Al box is illustrated in Figure 2b by comparing it with the temperatures from the baseline (bare Al box) and the ambient environment. All recorded temperatures increase in tandem with increasing solar irradiation; however, the increase is notably more pronounced in the bare Al box. At 10:19 AM, the maximum cooling differential between the coated Al box and the baseline reached 7.9 °C, primarily due to the high reflectivity of the paint in the visible and NIR regions.

During peak solar radiation hours, the RC paint-coated box registers temperatures exceeding the ambient, but the peak difference is limited to 2.1 °C at 10:44 AM. Subambient cooling is evident before 9:00 AM and after 4:00 PM during daytime, as well as during night-time, as shown in Figure 2c, but it is not observed during peak solar radiation hours. This behavior aligns with Mumbai's high relative humidity levels and ambient temperature, which effectively "close" the ATW. This effect of humidity on the RC cooling capacity is discussed in detail in Section 2.2.3.

2.2.2. Cooling Performance in Moderate Humid Conditions: Nagpur and Prayagraj. The cooling performance of TiO_2/PDMS paint was also tested in Nagpur, Maharashtra, and Prayagraj, Uttar Pradesh, in India. These tests were conducted in June, just before the onset of the monsoons. As a result, humidity and cloud presence were higher compared to peak summer conditions, though still lower than in Mumbai. Figure 3a shows the temperature of Al boxes, and Figure 3b shows global radiation recorded in Nagpur on June 12, 2023. The average humidity was 42%. Clouds passing over the sun explain the dips in solar radiation (Figure 3b). The temperature profile of the RC paint-coated Al box more or less overlaps with that of the ambient temperature (Figure 3a). The maximum temperature difference observed between the RC paint-coated Al box and the bare Al box was 9.2 °C at 12:39 PM, higher than what was observed in Mumbai. Similar results were observed in Prayagraj on June 22, 2023, with an average humidity of 45% (Figure 4). The maximum cooling performance of 8.1 °C for the RC paint-coated Al box, compared to the bare Al box, was observed in Prayagraj at 10:47 AM.

2.2.3. Theoretical Modeling: Effect of Humidity. The atmospheric conditions of the local environment strongly impact the cooling performance of the RC coating. An increase in humidity and air temperature reduces atmospheric transparency in the 8−13 μm wavelength range,[23] which in turn reduces the ability of the coating to radiate heat to outer space via the ATW. Consequently, the cooling performance of an RC

https://doi.org/10.1021/acsomega.4c07223
ACS Omega 2024, 9, 49494−49502

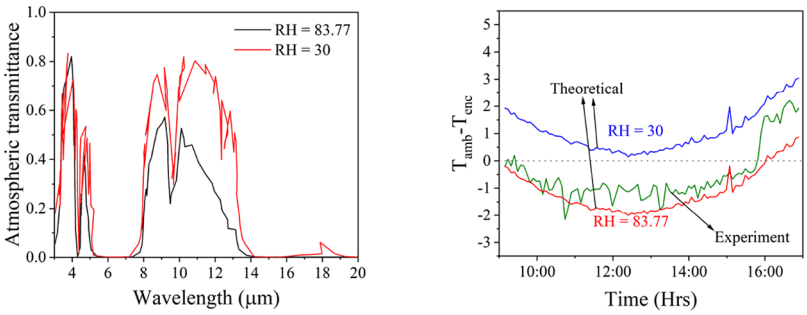

Figure 5. (a) Atmospheric transmittance calculated using MODTRAN for two RH viz. 30 and 83.77%. (b) Comparison between theoretical predictions and experimental measurements of $T_{amb} - T_{enc}$.

coating reduces significantly in high-humid environments. Herein, we aim to theoretically calculate the effect of humidity on the cooling performance of the RC coating and compare it with our experimental results. The calculations have been done by selecting the highly humid city of Mumbai, India, as the location. We use MODTRAN,[46] a widely used software for simulating the transmission of electromagnetic radiation through the Earth's atmosphere. This tool takes precipitable water vapor (PWV) as a key input to compute atmospheric transmittance. We follow the methodology reported by Dong et al.[21] to derive PWV values from relative humidity (RH) and ambient temperature data. A detailed description of this procedure is included in Section S2 of the Supporting Information. The calculations presented in this section are carried out for atmospheric parameters prevalent on April 25, 2023: 83.77% average humidity and 29.55 °C average ambient temperature, obtained from the Central Pollution Control Board (CPCB) portal.[47] Figure 5a shows the atmospheric transmittance calculated using MODTRAN under these ambient conditions, i.e., a corresponding PWV value of 5.54 cm. These parameters are then utilized in the standard energy balance equation applicable for radiative cooling systems. The energy balance equation equates the power radiated by the coating (P_{rad}) to the total heat gained by the coating (P_{loss}). The total heat gained by the coating consists of solar radiation losses (P_{sun}), atmospheric radiation losses (P_{atm}), and non-radiative heat losses ($P_{cond+conv}$). It is assumed that solar radiation is incident normally on the coating, while radiation emitted by the coating and the atmosphere is isotropic. Based on these assumptions, the following equations hold[8,39]:

$$P_{rad} = A\pi \int_0^\infty \epsilon(\lambda) I_{bb}(T_c, \lambda) d\lambda \quad (1)$$

$$P_{sun} = A \int_0^\infty \epsilon(\lambda) I_{AM1.5}(\lambda) d\lambda \quad (2)$$

$$P_{atm} = A\pi \int_0^\infty \epsilon(\lambda) \epsilon_{atm}(\lambda) I_{bb}(T_{amb}, \lambda) d\lambda \quad (3)$$

Here, $\epsilon(\lambda)$ is the emissivity of the paint coating; ϵ_{atm} is the emissivity of the atmosphere that is given by $\epsilon_{atm} = 1 - \tau^{1/\cos\theta}$, where τ is the atmospheric transmittance, and θ (assumed to be zero for this work) is the angle of incidence; and $I_{bb}(T_c, \lambda)$ and $I_{bb}(T_{amb}, \lambda)$ are the spectral blackbody radiation at the coating temperature T_c and ambient temperature T_{amb}, respectively, A is the cross-sectional area of the coating. Also, emissivity is calculated as $1 - R(\lambda)$ (R = spectral reflectivity). However, unlike other studies that focus on measuring the temperature of the coating, this work focuses on measuring the more practical enclosure temperature. Consequently, the nonradiative heat loss in the energy balance equation needs more careful consideration. The nonradiative heat loss, $P_{cond+conv}$, from the paint coating includes both losses to the ambient as well as to the Al box enclosure and can be quantified using

$$P_{cond+conv} = h_o(T_{amb} - T_c) + h_{c\text{-}Al}(T_{enc} - T_c) \quad (4)$$

where the coating temperature, T_c, and interior temperature of the Al box, T_{enc}, are related by

$$h_{eff}(T_{amb} - T_{enc}) = h_{c\text{-}Al}(T_{enc} - T_c) \quad (5)$$

Here, h_0 (=10.43 $Wm^{2-}K^{-1}$) is the external convective heat transfer coefficient estimated using empirical relations[48] based on the prevalent wind speed on that day, T_{amb} is the ambient temperature, $h_{c\text{-}Al}$ is the effective heat transfer coefficient between the coating surface and still-air in the enclosure of the Al box, and h_{eff} is the overall effective heat transfer coefficient of the setup from the enclosure space to the ambient, which can be quantified using

$$\frac{1}{h_{eff}} = \frac{1}{h_o} + \frac{l_c}{k_c} + \frac{1}{h_{c\text{-}Al}} \quad (6)$$

and

$$\frac{1}{h_{c\text{-}Al}} = \frac{l_{Al}}{k_{Al}} + TBR + \frac{1}{h_i} \quad (7)$$

Here, l_c and k_c represent the thickness and thermal conductivity of the RC paint, respectively, while l_{Al} = 4 mm and k_{Al} = 237 Wm^{-1} K^{-1} are those of the Al wall, with h_i denoting internal heat transfer between the still-air and the Al wall. The thermal barrier resistance (TBR) between the polymer coating and the Al surface[49,50] and the thermal resistance due to the Al wall are both assumed to be small compared to $1/h_i$ and are hence neglected. A standard value of 2.6 $Wm^{2-}K^{-1}$ is used for the internal heat transfer coefficient.[51,52] The value k_c is obtained from Maxwell's relation[53] $k_c = k_m\,(1 + 3f/((k_p + 2k_m)/(k_p - k_m) - f))$, where subscript m stands for the matrix, and p stands for the particle. The thermal conductivities of PDMS and TiO_2 are taken to be k_m = 0.2 $Wm^{-1}K^{-1}$ and k_p = 4.8 $Wm^{-1}K^{-1}$, respectively.

Using the atmospheric transmittance from Figure 5a and with the conduction and convection heat losses obtained from eq 4, we calculate the equilibrium temperature of the enclosure space of the RC paint-coated Al box, T_{enc}, by solving the energy balance equation ($P_{rad} - P_{sun} - P_{atm} - P_{cond+conv} = 0$).

https://doi.org/10.1021/acsomega.4c07223
ACS Omega 2024, 9, 49494−49502

The deviation of T_{enc} from the measured ambient temperature, an indicator of the cooling performance of the RC coating, is plotted in Figure 5b and compared to experimental measurements. An appreciable match with the experimental measurements is observed. Figure 5b also contrasts the cooling performance under low humidity conditions (RH = 30%). Other parameters, such as ambient temperature and the heat transfer coefficient, are left untouched. A marked decrease in the cooling performance is noted in Figure 5b with increased humidity levels. It can thus be inferred that RC coatings deployed in highly humid regions will experience an appreciable drop in their emissive performance, translating to difficulties in achieving subambient cooling. This aligns with our experimental findings.

Although the TiO_2/PDMS-based RC coating is not able to provide subambient cooling in highly humid environments, it does help reduce the internal temperature of an enclosure significantly. Since the goal of developing such material coatings is to minimize reliance on energy-consuming cooling systems like air conditioners, achieving subambient temperatures should not be the sole criterion for evaluating RC coating efficiency. Instead, measuring temperature reductions in comparison to a standard control, while also considering prevailing atmospheric conditions, provides a more relevant benchmark.

2.3. Impact of Experimental Factors on Subambient Cooling. Apart from environmental factors, experimental factors like the use of a PE cover and the measurement of ambient temperature can have a significant impact on the cooling performances observed for RC coatings. The adoption of inaccurate methodologies can yield misleading numbers for cooling performance. In the following sections, we shall discuss how the configuration of the experimental setup influences the observations of the cooling efficiency of an RC coating.

2.3.1. Ambiguity in the Measurement of the Ambient Temperature. The performance of the RC coating is usually evaluated by comparing the temperature of the coating with the ambient temperature. Therefore, inaccurate measurement of ambient temperature can lead to misleading conclusions about the coating's cooling performance. Standard methods for measuring ambient temperature frequently rely on thermocouples exposed to environmental factors such as sunlight and wind,[12,15,26,54] leading to potential fluctuations and inaccuracies in the readings. A more reliable alternative is the use of a Stevenson screen, as shown in Figure 2a, which serves as a shield against radiation and wind, providing more stable measurements. This shield minimizes exposure to the sun and regulates airflow, enabling more precise and consistent measurements. The importance of tools such as the Stevenson screen is underscored by its impact on evaluating cooling performance. For instance, Figure 6 shows two ambient temperatures: one measured by a thermocouple placed inside the Stevenson screen and another exposed to the sun and wind. The former measures lower ambient temperatures during the day. The opposite is observed at night, owing to cooler winds. Figure 6 also presents the temperature profile for an RC paint-coated aluminum box. Measurements using an unshielded/exposed thermocouple would inaccurately suggest that the paint cools below ambient temperatures during the day, in total contrast to the measurements from the shielded thermocouple. Accurate ambient temperature measurement is thus critical for reporting reliable subambient cooling, and

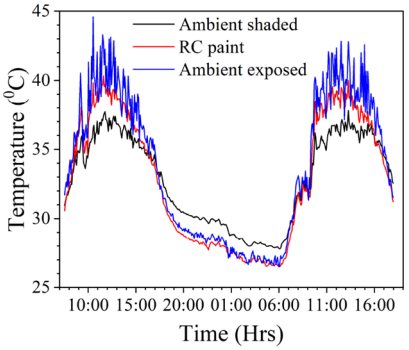

Figure 6. Comparison of the temperature of RC paint and ambient temperature. Here, "Ambient shaded" is the ambient temperature measured by the Stevenson screen, whereas "Ambient exposed" is the ambient temperature measured by a thermocouple exposed to the sun and wind. The data were recorded on May 21−22, 2023.

shielded thermocouples (if not devices) are highly recommended for consistent RC coating performance evaluation.

2.3.2. Using Polyethylene Sheet as a Convection Shield. The cooling performance of the RC coating is greatly affected by conduction and convection losses. To address this, studies report the use of a radiation shield with a polyethylene (PE) film covering on the top side to counter these parasitic losses.[2,8,15,35,55] The radiation shield, which is typically made of aluminum foil, keeps the coating directly facing the sky, while the PE film controls convective heat loss. In an experiment designed to assess the impact of this configuration, we recorded temperatures from an RC paint-coated aluminum (Al) box, a bare Al box, and the air within a polyethylene (PE)-covered setup, as shown in Figure 7a. The results, shown in Figure 7b, indicate a notable increase in both the air temperature inside the PE-covered setup and the enclosure temperature of the bare Al box. This facilitated the observation of subambient cooling throughout the day, with a maximum cooling of 11.5 °C below ambient and 21.4 °C compared to the uncoated Al box. The PE top-cover film, while reducing convective heat loss, traps heat, raising the air temperature in the PE-covered setup to 60−70 °C. Hence, the use of top-cover PE films as convective shields is not recommended for measuring cooling performance, as they can significantly skew the results. However, PE films can be used as side-cover convection shields for the enclosure testing of RC coatings, while the top is kept open. For such designs, provided the height of the sides is sufficient to limit forced convection, the inflation of temperature discussed above will not be observed.[56]

3. CONCLUSIONS

This study tested the performance of a low particle volume fraction TiO_2/PDMS paint coating designed for passive daytime radiative cooling in a tropical environment. The paint exhibits high reflectivity of 94% in the visible and near-IR spectra and an emissivity of 92.4% between 8 and 13 μm wavelengths. Instead of comparing the coated surface temperature with the ambient temperature, as commonly done in the literature, this study compares the enclosure temperature with the ambient temperature, offering greater practical utility for real-world applications. Although subambient cooling was not achieved, largely due to the highly humid environment limiting the effectiveness of radiative heat transfer via the atmospheric transparency window, the coating significantly reduced the

https://doi.org/10.1021/acsomega.4c07223
ACS Omega 2024, 9, 49494−49502

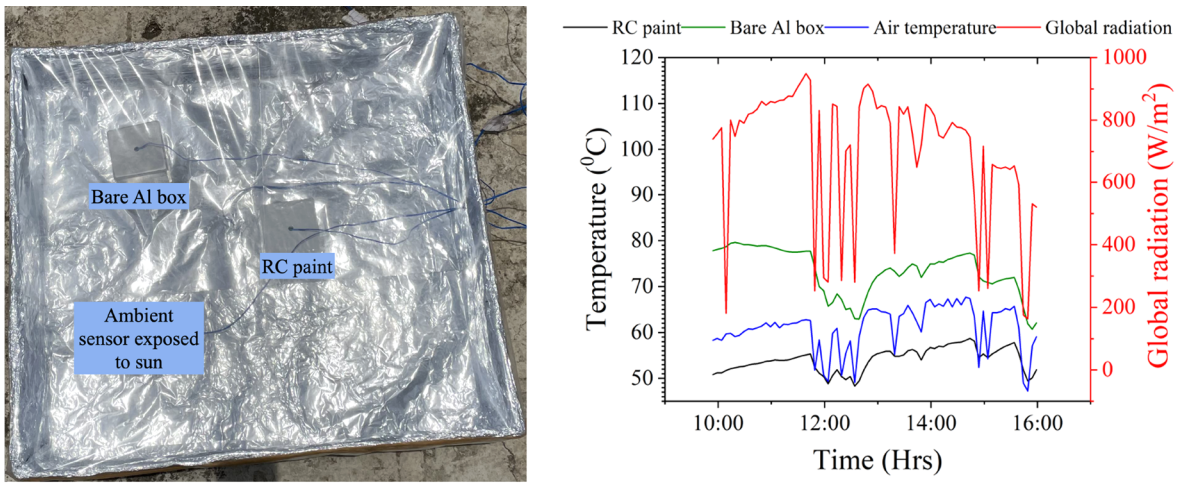

Figure 7. (a) Setup for testing cooling performance, incorporating a radiation shield and PE cover. (b) Temperature measurements of an RC paint-coated Al box, a bare Al box, and the air within the radiation-shielded box covered with PE, taken on June 11, 2023.

heat load in the enclosed space of a hollow aluminum box compared to an uncoated control. A maximum reduction of 7.9 °C in the internal temperature of the RC paint-coated aluminum (Al) box compared to the uncoated Al box was observed in a highly humid environment, and a 9.2 °C reduction was observed in a moderately humid environment. With the primary goal to minimize energy consumption for space cooling, these outdoor experiments show that TiO_2-based RC coatings have the potential to be used in tropical conditions. The study has also highlighted methodologies presently used to evaluate and report cooling performance, specifically the measurement of ambient temperature with sensors exposed to sunlight and wind alongside the use of polyethylene sheets as convective barriers. Through experimental observations, we find that these approaches to characterize the cooling performance of RC coatings could yield misleading conclusions regarding their subambient cooling capabilities. This study strongly suggests the reporting of prevalent climatic conditions during outdoor tests and the use of shielded thermocouples for ambient temperature measurements and cautions against the use of top-covered convection shields.

4. EXPERIMENTAL SECTION

4.1. Fabrication of RC Paint. The TiO_2 and o-Xylene were sourced from Sigma-Adlrich, whereas PDMS (SYLGARD 184) was sourced from Dow. The binder (PDMS), solvent (o-Xylene), and pigment (TiO_2) were mixed using a mechanical stirrer. 70% of the PDMS to be used in the formulation was mixed with o-Xylene in a 1:1 ratio, and stirring at 200 rpm gave a clear solution. TiO_2 pigment was then added under slow stirring and then increased stirring to 500 rpm for 30 min. In the same ratio, the remaining PDMS and o-Xylene were subsequently added and stirred for 90 min. After resting the solution overnight, we applied two coats to aluminum substrates, allowing a 24 h curing period at room temperature. The two-coat procedure gives an average thickness of 280 μm ± 30 μm. We observe that o-Xylene can be added at any stage to adjust the viscosity without affecting the optical properties.

4.2. Characterization of the Coating. We employed a field emission scanning electron microscope (Zeiss Ultra 55) to image and characterize the pigment powder particles. The spectral reflectivity of the developed coating in the 0.3−2.5 μm wavelength range was characterized using a PerkinElmer Lambda 950 UV-vis-NIR spectrometer with a 150 mm integrating sphere, and in the 2.5−18 μm range using a PerkinElmer Frontier FTIR spectrometer with a 75 mm integrating sphere. The sample's reflectivity in the 0.3−2.5 μm wavelength range was measured against a Spectralon reflectance standard and then adjusted by multiplying with the standard's reflectivity (Figure S3 in the Supporting Information) to obtain the absolute reflectivity of the TiO_2/PDMS coating. The thickness of the coating was measured by using a Fujitech DFT gauge.

4.3. Experimental Setup for Cooling Performance Measurement of the Coating. The paint was applied to the box's exterior with a brush, and a top hole was created to accommodate a thermocouple (sealed with cotton wool) to measure the internal temperature of the box. We used a Keysight DAQ970A data logger to record temperature data from T-type thermocouples at regular intervals. Each thermocouple was calibrated with a Julabo calibration bath. The thermocouples are immersed in the water bath, and the bath temperature was increased from ambient temperature to 90 °C at intervals of 5 °C. Temperatures of the thermocouples and the bath were recorded simultaneously. Subsequently, an empirical relation for temperature was obtained for each thermocouple to calculate its respective calibrated temperature. Global solar irradiation at the experimental site was measured by using a Dynalab Weathertech pyranometer (model 147059). Ambient temperature was measured using a Stevenson screen from TrackSo, with an accuracy of ±0.5 °C.

■ ASSOCIATED CONTENT

Supporting Information

The Supporting Information is available free of charge at https://pubs.acs.org/doi/10.1021/acsomega.4c07223.

Design of paint coating; calculation of atmospheric transmittance using MODTRAN; refractive indices of TiO_2 and PDMS; simulated reflectivity of TiO_2/PDMS coating for various radius of particles and volume

https://doi.org/10.1021/acsomega.4c07223
ACS Omega 2024, 9, 49494−49502

fractions; and reflectivity of the Spectralon reflectance standard (PDF)

AUTHOR INFORMATION

Corresponding Author

Karthik Sasihithlu − *Department of Energy Science and Engineering, Indian Institute of Technology Bombay, Mumbai 400076 Maharashtra, India;* orcid.org/0000-0002-6894-8186; Email: ksasihithlu@iitb.ac.in

Authors

Bhrigu Rishi Mishra − *Department of Energy Science and Engineering, Indian Institute of Technology Bombay, Mumbai 400076 Maharashtra, India;* orcid.org/0000-0002-1900-7603

Sreerag Sundaram − *Department of Energy Science and Engineering, Indian Institute of Technology Bombay, Mumbai 400076 Maharashtra, India;* orcid.org/0000-0001-6002-8193

Complete contact information is available at: https://pubs.acs.org/10.1021/acsomega.4c07223

Author Contributions

‡Joint first authors.

Author Contributions

B.R.M.: conceptualization, data curation, investigation, methodology, validation, and writing - original draft. S.S.: conceptualization, investigation, methodology, validation, and writing - original draft. K.S.: conceptualization, supervision, investigation, funding acquisition, and writing - review and editing.

Notes

The authors declare no competing financial interest.

ACKNOWLEDGMENTS

B.R.M. and S.S. acknowledge support from Prime Minister's Research Fellowship (PMRF). K.S. acknowledges support from La Fondation Dassault Systèmes and SERB Grant No. SRG/2020/001 511. The authors thank P.P. Joshi from Thermogreen Cool Coat Pvt. Ltd. for his valuable guidance in paint development. The authors are also thankful to Dr. H.C. Barshilia from CSIR-National Aerospace Laboratories, Bangalore, India, from whom the results from the FTIR setup were obtained.

REFERENCES

(1) Mandal, J.; Yang, Y.; Yu, N.; Raman, A. Paints as a scalable and effective radiative cooling technology for buildings. *Joule* **2020**, *4*, 1350−1356.

(2) Li, X.; Peoples, J.; Yao, P.; Ruan, X. Ultrawhite $BaSO_4$ Paints and Films for Remarkable Daytime Subambient Radiative Cooling. *ACS Appl. Mater. Interfaces* **2021**, *13*, 21733−21739.

(3) Wu, T.; Han, L.; Wu, Q.; Li, H.; Ning, S.; Zhou, L.; Zhang, S.; Zheng, H.; Jia, B. Design of radiative cooling covers for automobiles with maximized cooling power. *Int. J. Heat Mass Transf.* **2024**, *227*, No. 125601.

(4) Li, J.; Fu, Y.; Zhou, J.; Yao, K.; Ma, X.; Gao, S.; Wang, Z.; Dai, J.-G.; Lei, D.; Yu, X. Ultrathin, soft, radiative cooling interfaces for advanced thermal management in skin electronics. *Sci. Adv.* **2023**, *9*, No. eadg1837.

(5) Chen, Z.; Zhu, L.; Raman, A.; Fan, S. Radiative cooling to deep sub-freezing temperatures through a 24-h day-nightt cycle. *Nat. Commun.* **2016**, *7*, 13729.

(6) So, S.; Yun, J.; Ko, B.; Lee, D.; Kim, M.; Noh, J.; Park, C.; Park, J.; Rho, J. Radiative cooling for energy sustainability: from fundamentals to fabrication methods toward commercialization. *Adv. Sci.* **2024**, *11*, No. 2305067.

(7) Bijarniya, J. P.; Tripathi, S.; Bauri, S.; Sarkar, J.; Maiti, P. Progress on Natural and Sustainable Materials for Daytime Radiative Cooling. *ACS Appl. Opt. Mater.* **2024**, *2*, 945−962.

(8) Raman, A.; Anoma, M.; Zhu, L.; Rephaeli, E.; Fan, S. Passive radiative cooling below ambient air temperature under direct sunlight. *Nature* **2014**, *515*, 540−544.

(9) Zhai, Y.; Ma, Y.; David, S.; Zhao, D.; Lou, R.; Tan, G.; Yang, R.; Yin, X. Scalable-manufactured randomized glass-polymer hybrid metamaterial for daytime radiative cooling. *Science* **2017**, *355*, 1062−1066.

(10) Zhang, H.; Ly, K.; Liu, X.; Chen, Z.; Yan, M.; Wu, Z.; Wang, X.; Zheng, Y.; Zhou, H.; Fan, T. Biologically inspired flexible photonic films for efficient passive radiative cooling. *Proc. Natl. Acad. Sci. U. S. A.* **2020**, *117*, 14657−14666.

(11) Liu, X.; Xiao, C.; Wang, P.; Yan, M.; Wang, H.; Xie, P.; Liu, G.; Zhou, H.; Zhang, D.; Fan, T. Biomimetic photonic multiform composite for high-performance radiative cooling. *Adv. Opt. Mater.* **2021**, *9*, No. 2101151.

(12) Mandal, J.; Fu, Y.; Overvig, A.; Jia, M.; Sun, K.; Shi, N.; Zhou, H.; Xiao, X.; Yu, N.; Yang, Y. Hierarchically porous polymer coatings for highly efficient passive daytime radiative cooling. *Science* **2018**, *362*, 315−319.

(13) Atiganyanun, S.; Plumley, J.; Han, S.; Hsu, K.; Cytrynbaum, J.; Peng, T.; Han, S.; Han, S. Effective radiative cooling by paint-format microsphere-based photonic random media. *ACS Photonics* **2018**, *5*, 1181−1187.

(14) Li, X.; Peoples, J.; Huang, Z.; Zhao, Z.; Qiu, J.; Ruan, X. Full daytime sub-ambient radiative cooling in commercial-like paints with high figure of merit. *Cell Reports Physical Science* **2020**, *1*, No. 100221.

(15) Zhang, Y.; Tan, X.; Qi, G.; Yang, X.; Hu, D.; Fyffe, P.; Chen, X. Effective radiative cooling with ZrO_2/PDMS reflective coating. *Sol. Energy Mater. Sol. Cells* **2021**, *229*, No. 111129.

(16) Xue, X.; et al. Creating an eco-friendly builing coating with smart subambient raidative cooling. *Adv. Mater.* **2020**, *32*, No. 1906751.

(17) Zhang, L.; Zhan, H.; Xia, Y.; Zhang, R.; Xue, J.; Yong, J.; Zhao, L.; Liu, Y.; Feng, S. Efficient Passive Daytime Radiative Cooling by Hierarchically Designed Films Integrating Robust Durability. *ACS Appl. Mater. Interfaces* **2023**, *15*, 31994−32001.

(18) Liu, S.; Zhang, F.; Chen, X.; Yan, H.; Chen, W.; Chen, M. Thin paints for durable and scalable radiative cooling. *Journal of Energy Chemistry* **2024**, *90*, 176−182.

(19) Guo, N.; Shi, C.; Warren, N.; Sprague-Klein, E. A.; Sheldon, B. W.; Yan, H.; Chen, M. Challenges and Opportunities for Passive Thermoregulation. *Adv. Energy Mater.* **20241**, *14*, No. 2401776.

(20) Liu, C.; Wu, Y.; Wang, B.; Zhao, C.; Bao, H. Effect of atmospheric water vapor on radiative cooling performance of different surfaces. *Sol. Energy* **2019**, *183*, 218−225.

(21) Dong, M.; Chen, N.; Zhao, X.; Fan, S.; Chen, Z. Nighttime radiative cooling in hot and humid climates. *Opt. Express* **2019**, *27*, 31587−31598.

(22) Bijarniya, J.; Sarkar, J.; Maiti, P. Environmental effect on the performance of passive daytime photonic radiative cooling and building energy-saving potential. *Journal of Cleaner Production* **2020**, *274*, No. 123119.

(23) Song, X.; Gao, Y.; Farooq, A.; Zhang, P. Temperature non-uniformity in the radiative cooler and its effect on performance under various humidity conditions. *Sol. Energy* **2021**, *220*, 498−508.

(24) Huang, J.; Lin, C.; Li, Y.; Huang, B. Effects of humidity, aerosol, and cloud on subambient radiative cooling. *Int. J. Heat Mass Transfer* **2022**, *186*, No. 122438.

(25) Jeong, S.; Tso, C. Y.; Wong, Y. M.; Chao, C. Y.; Huang, B. Daytime passive radiative cooling by ultra emissive bio-inspired polymeric surface. *Sol. Energy Mater. Sol. Cells* **2020**, *206*, No. 110296.

(26) Zhong, H.; Zhang, P.; Li, Y.; Yang, X.; Zhao, Y.; Wang, Z. Highly solar-reflective structures for daytime radiative cooling under high humidity. *ACS Appl. Mater. Interfaces* **2020**, *12*, 51409−51417.
(27) Gao, Y.; Song, X.; Farooq, A. S.; Zhang, P. Cooling performance of porous polymer radiative coating under different environmental conditions throughout all-year. *Sol. Energy* **2021**, *228*, 474−485.
(28) Han, D.; Fei, J.; Mandal, J.; Liu, Z.; Li, H.; Raman, A. P.; Ng, B. F. Sub-ambient radiative cooling under tropical climate using highly reflective polymeric coating. *Sol. Energy Mater. Sol. Cells* **2022**, *240*, No. 111723.
(29) Wijewardane, S. Inventions, innovations, and new technologies: Paints and coatings for passive cooling. *Solar Compass* **2022**, *3*, No. 100032.
(30) Rooney, M. Effect of Pigment Volume Concentration on Physical and Chemical Properties of Acrylic Emulsion Paints Assessed using Single-Sided Nmr; Dissertations, Theses, and Masters Projects; William & Mary, 2018.
(31) Rodrıguez, M.; Gracenea, J.; Kudama, A.; Suay, J. The influence of pigment volume concentration (PVC) on the properties of an epoxy coating: Part I. Thermal and mechanical properties. *Prog. Org. Coat.* **2004**, *50*, 62−67.
(32) Kasyanenko, I.; Kramarenko, V. The effect of pigment volume concentration on film formation and the mechanical properties of coatings based on water-dispersion paint and varnish materials. *Mechanics of Composite Materials* **2018**, *53*, 767−780.
(33) Bijarniya, J. P.; Sarkar, J.; Tiwari, S.; Maiti, P. Development and degradation analysis of novel three-layered sustainable composite coating for daytime radiative cooling. *Sol. Energy Mater. Sol. Cells* **2023**, *257*, No. 112386.
(34) Song, J.; Zhang, W.; Sun, Z.; Pan, M.; Tian, F.; Li, X.; Ye, M.; Deng, X. Durable radiative cooling against environmental aging. *Nat. Commun.* **2022**, *13*, 4805.
(35) Du, T.; Niu, J.; Wang, L.; Bai, J.; Wang, S.; Li, S.; Fan, Y. Daytime Radiative Cooling Coating Based on the Y2O3/TiO2Microparticle-Embedded PDMS Polymer on Energy-Saving Buildings. *ACS Appl. Mater. Interfaces* **2022**, *14*, 51351−51360.
(36) Lin, K.; Zhu, T.; Zhu, Y.; Ho, T. C.; Lee, H. H.; Chao, L.; Tso, C. Y. A Dual-Layer Coating Using Nanoparticle-Polymer Hybrid Materials for Daytime Passive Radiative Cooling. In *ASME Power Conference*; American Society of Mechanical Engineers, 2022, p. V001T07A003.
(37) Jung, J.; Yoon, S.; Kim, B.; Kim, J. B. Development of High-Performance Flexible Radiative Cooling Film Using PDMS/TiO2Microparticles. *Micromachines* **2023**, *14*, 2223.
(38) Atiganyanun, S. Use of hollow silica and titanium dioxide microparticles in solar reflective paints for daytime radiative cooling applications in a tropical region. *Journal of Photonics for Energy* **2021**, *11*, No. 022103.
(39) Mishra, B. R.; Sundaram, S.; Varghese, N. J.; Sasihithlu, K. Disordered metamaterial coating for daytime passive radiative cooling. *AIP Adv.* **2021**, *11*, 105218.
(40) Xia, S.; Wang, F.; Yang, S.; Long, H.; Ju, H.; Ou, J. Water-based kaolin/polyacrylate cooling paint for exterior walls. *Colloids Surf., A* **2023**, *677*, No. 132401.
(41) Zhou, L.; Yin, X.; Gan, Q. Best practices for radiative cooling. *Nature Sustainability* **2023**, *6*, 1030−1032.
(42) Bu, K.; Huang, X.; Li, X.; Bao, H. Consistent Assessment of the Cooling Performance of Radiative Cooling Materials. *Adv. Funct. Mater.* **2023**, *33*, No. 2307191.
(43) ASTM International. ASTM G173−03, Standard Tables for Reference Solar Spectral Irradiances: Direct Normal and Hemispherical on 37° Tilted Surface, 2012.
(44) Bijarniya, J.; Sarkar, J.; Tiwari, S.; Maiti, P. Experimentally optimized particle−polymer matrix structure for efficient daytime radiative cooling. *J. Renew. Sustainable Energy* **2022**, *14*, No. 055101.
(45) Das, P.; Rudra, S.; Maurya, K.; Saha, B. Ultra-Emissive MgO-PVDF Polymer Nanocomposite Paint for Passive Daytime Radiative Cooling. *Adv. Mater. Technol.* **2023**, *8*, No. 2301174.
(46) MODTRAN. http://modtran.spectral.com/modtran_home#plot (accessed September 23, 2024).
(47) Central Pollution Control Board. https://airquality.cpcb.gov.in/ccr/#/caaqm-dashboard-all/caaqm-landing/data (accessed September 23, 2024).
(48) Test, F.; Lessmann, R.; Johary, A. Heat transfer during wind flow over rectangular bodies in the natural environment. *Journal of Heat Transfer, Trans. ASME* **1981**, *103*, 262−267.
(49) Fuller, J.; Marotta, E. Thermal contact conductance of metal/polymer joints: an analytical and experimental investigation. *Journal of thermophysics and heat transfer* **2001**, *15*, 228−238.
(50) Bendada, A.; Derdouri, A.; Lamontagne, M.; Simard, Y. Analysis of thermal contact resistance between polymer and mold in injection molding. *Applied thermal engineering* **2004**, *24*, 2029−2040.
(51) Qengel, Y.; Ghajar, A. *Heat and Mass Transfer: Fundamental and Applications*; McGraw Hill, 2014.
(52) Gerlich, V. *Modelling Of Heat Transfer In Buildings*; ECMS, 2011; pp. 244−248.
(53) Maxwell, J. *A Treatise on Electricity and Magnetism*; Clarendon Press, 1873.
(54) Wang, T.; Wu, Y.; Shi, L.; Hu, X.; Chen, M.; Wu, L. A structural polymer for highly efficient all-day passive radiative cooling. *Nat. Commun.* **2018**, *12*, 365.
(55) Kou, J.; Jurado, Z.; Chen, Z.; Fan, S.; Minnich, A. Daytime radiative cooling using near-black infrared emitters. *ACS Photonics* **2017**, *4*, 626−630.
(56) Felicelli, A.; Wang, J.; Feng, D.; Forti, E.; Azrak, S. E. A.; Peoples, J.; Youngblood, J.; Chiu, G.; Ruan, X. Efficient radiative cooling of low-cost BaSO4 paint-paper dual-layer thin films. *Nanophotonics* **2024**, *13*, 639−648.

https://doi.org/10.1021/acsomega.4c07223
ACS Omega 2024, 9, 49494−49502